Comparative Analysis of Effective Stiffness Models for Immediate Deflection Prediction in Reinforced Concrete Beams

Rafael Hofstätter Azambuja
Independent researcher, Pelotas, Rio Grande do Sul, Brazil

ABSTRACT

Objective: To quantify how effective-stiffness models affect immediate deflection estimates for reinforced concrete beams. **Methodology:** The Branson, rational Bischoff, and ACI 318-19 formulations were evaluated for rectangular sections with reinforcement ratios of 0.30–2.00% and applied-to-cracking moment ratios of 1.0–4.0, totaling 1,098 evaluations. **Results:** Divergence peaked immediately after cracking and at low reinforcement ratios; ACI 318-19 predicted lower stiffness and larger deflection than Branson over almost the entire domain, the only exception being a negligible reversal (below 0.1%) for the most heavily reinforced section at the highest load ratios. **Limitations:** No experimental database or long-term effects were considered. **Originality:** Dimensionless maps identify regions sensitive to model choice. **Conclusions:** The cracking moment, gross and cracked inertias, and adopted equation should be reported.

Keywords: reinforced concrete; serviceability; immediate deflection; effective inertia; cracking.

1 INTRODUCTION

Deflection control is often decisive in the design of reinforced concrete members, even when strength requirements are satisfied. Excessive displacements can damage partitions and finishes, impair drainage, produce visually unacceptable floors, and reduce occupant confidence. Unlike the flexural strength problem, the stiffness of a reinforced concrete beam under service loads is not adequately represented by a single elastic section property.

Before cracking, the gross concrete section contributes to flexural stiffness. After cracking, the tensioned concrete at the crack section is no longer effective, while the concrete between cracks continues to carry tensile stresses through bond with the reinforcement. The resulting response lies between the limits of the gross section and the fully cracked section, and it evolves with loading.

Design procedures frequently represent this distributed nonlinear response through an effective moment of inertia, I_e. Branson's empirical interpolation, developed from tests reported in the 1960s (Branson, 1963), became the basis of the deflection provisions of several codes. Its appeal is evident: a single scalar stiffness allows conventional elastic beam equations to be retained. Loading type, reinforcement ratio, time-dependent effects, and slab behavior are recognized as relevant to deflection prediction (Al-Zaid et al., 1991; Al-Shaikh and Al-Zaid, 1993; Gilbert, 1999; Scanlon and Murray, 1982).

Eurocode 2 follows a different route, interpolating curvatures or deflections between the uncracked and fully cracked states rather than interpolating the moment of inertia (European Committee for Standardization, 2004). Later research showed that cubic interpolation can overestimate stiffness when the reinforcement ratio is low or when the ratio I_g/I_{cr} is high (Bischoff, 2005; Bischoff, 2007; Bischoff and Scanlon, 2007). Bischoff (2005) proposed a rational alternative that incorporates the tension-stiffening model adopted in Europe, so that the tension-stiffening contribution no longer grows with I_g/I_{cr} as it does in Branson's equation, and developed it further for beams and slabs (Bischoff, 2007).

Scanlon and Bischoff (2008), evaluating an alternative effective-inertia formulation valid over a wide range of reinforcement ratios, recommended a cracking moment equal to two-thirds of the code value to account for shrinkage restraint stresses. The expression adopted by ACI 318-19 combines a rational interpolation of this kind with the reduced cracking moment (ACI Committee 318, 2019). The current

ACI approach therefore reduces the cracking moment used in the transition and increases the computed deflection relative to the former Branson formulation.

These formulations are sometimes treated as interchangeable computational details, but they are not. Because elastic deflection is inversely proportional to EI, even a moderate difference in effective inertia can move a member from one side of a serviceability limit to the other. This is particularly relevant when Brazilian calculations based on NBR 6118 (ABNT, 2023) are compared with North American software or checks based on ACI 318-19 (ACI Committee 318, 2019).

A direct comparison must separate two questions: how much the formulas diverge, and which of them better predicts tests. The first can be answered analytically; the second requires a representative experimental database and treatment of uncertainty.

This paper addresses the first question. Its objective is to quantify the sensitivity of immediate deflection estimates to the selected effective-stiffness model, considering practical ranges of longitudinal reinforcement and post-cracking loading. The contribution consists of normalized response curves and divergence maps that highlight the parametric regions in which model choice becomes relevant. The analysis is deliberately restricted to short-term monotonic bending of rectangular, non-prestressed, singly reinforced beams. Creep, shrinkage, cyclic loading, shear deformation, compression reinforcement, and loading-history effects are outside the scope.

2 THEORETICAL BACKGROUND

2.1 Section properties and cracking

For a rectangular section of width b and total depth h, the moment of inertia of the gross section is

$$I_g = \frac{bh^3}{12} \tag{1}$$

The cracking moment is conventionally related to the modulus of rupture f_r, the gross inertia, and the distance y_t from the centroid to the tension face:

$$M_{cr} = \frac{f_r I_g}{y_t} \tag{2}$$

The value of f_r depends on the code considered. In the present normalized study, the applied moment is introduced through $\lambda = M_a/M_{cr}$; therefore, the comparison is governed by the stiffness interpolation rather than by a specific national expression for tensile strength. For a singly reinforced rectangular section, the neutral-axis depth x of the transformed cracked section follows from the equilibrium of first moments of area:

$$\frac{bx^2}{2} = nA_s(d-x) \tag{3}$$

where $n = E_s/E_c$. Neglecting concrete in tension, the inertia of the transformed cracked section is

$$I_{cr} = \frac{bx^3}{3} + nA_s(d-x)^2 \tag{4}$$

These expressions isolate the influence of the reinforcement ratio on the stiffness contrast I_g/I_{cr}. A low reinforcement ratio produces a relatively small I_{cr} and therefore makes the interpolation between the uncracked and cracked states more relevant.

2.2 Branson model

Branson proposed a cubic interpolation between the gross and cracked inertias. For M_a greater than M_{cr}, the expression used in this study is

$$I_{e,B} = \left(\frac{M_{cr}}{M_a}\right)^3 I_g + \left[1 - \left(\frac{M_{cr}}{M_a}\right)^3\right] I_{cr} \leq I_g \tag{5}$$

For $M_a \leq M_{cr}$, $I_e = I_g$. The exponent of three causes a relatively rapid reduction in the contribution of the uncracked section as the applied moment increases. Bischoff (2007) notes that the equation works well within a narrow range corresponding to steel-reinforced beams with reinforcement ratios between about 1% and 2%, and Bischoff and Scanlon (2007) found that it overestimates member stiffness at lower reinforcement ratios.

2.3 Rational Bischoff model

The rational formulation expresses the effective inertia through a flexibility-based interpolation:

$$I_{e,R} = \frac{I_{cr}}{1 - \left(\frac{M_{cr}}{M_a}\right)^2 \left(1 - \frac{I_{cr}}{I_g}\right)} \leq I_g \tag{6}$$

This form approaches I_g at cracking and I_{cr} at high load levels. Because tension stiffening is measured relative to the fully cracked response, the expression does not reproduce the overestimation of tension stiffening that the cubic expression exhibits at high I_g/I_{cr} ratios (Bischoff, 2005), and it is therefore less prone to retain excessive stiffness in such members.

Published assessments have associated this behavior with a better representation of members with low steel reinforcement ratios and of members reinforced with lower-modulus fiber-reinforced polymer bars (Bischoff, 2005; Bischoff, 2007; Bischoff and Scanlon, 2007).

2.4 ACI 318-19 model

ACI 318-19 replaced the former Branson equation with a rational expression and uses two-thirds of the computed cracking moment in the transition (ACI Committee 318, 2019):

$$I_{e,A} = \frac{I_{cr}}{1 - \left(\frac{(2/3)M_{cr}}{M_a}\right)^2 \left(1 - \frac{I_{cr}}{I_g}\right)} \tag{7}$$

For $M_a \leq (2/3)M_{cr}$, the gross inertia is used. The reduced threshold accounts for tensile stresses that develop in the concrete from restraint of shrinkage by the reinforcement, which lower the moment at which flexural cracking actually occurs (Scanlon and Bischoff, 2008). Consequently, this formulation yields a lower I_e than the unreduced rational model throughout the domain and a lower I_e than the Branson equation at the onset of the post-cracking regime.

3 METHODOLOGY

3.1 Reference section and parametric domain

A rectangular beam section was selected to provide a transparent numerical reference. A width of 300 mm, total depth of 500 mm, effective depth of 450 mm, concrete compressive strength of 30 MPa,

and steel modulus of elasticity of 200 GPa were adopted. The concrete modulus of elasticity was computed as $E_c = 5600\sqrt{f_{ck}}$ MPa, the NBR 6118 initial tangent modulus for granite or gneiss aggregate (ABNT, 2023), solely to establish the modular ratio ($n = 6.52$) and the transformed cracked section.

This choice is a reference assumption, not a code requirement: the equivalent-stiffness expression of NBR 6118 is written in terms of the secant modulus E_{cs}, and ACI 318-19 uses $E_c = 4700\sqrt{f'_c}$. Both give a larger modular ratio ($n \approx 7.45$ and 7.77, respectively), a larger I_{cr}/I_g, and therefore smaller divergences; for example, the ACI–Branson difference at $\rho = 0.30\%$ and $M_a/M_{cr} = 1.10$ falls from 304% with E_{ci} to 265% with E_{cs}. The trends reported below are unchanged by this choice.

Six tension reinforcement ratios, defined by $\rho = A_s/(bd)$, were considered: 0.30%, 0.50%, 0.75%, 1.00%, 1.50%, and 2.00%. The ratio λ between the applied moment and the cracking moment ranged from 1.00 to 4.00 in increments of 0.05, resulting in 366 section–load combinations and 1,098 model evaluations.

Table 1. Reference section and parametric domain

Parameter	Symbol	Values	Unit
Width	b	300	mm
Total depth	h	500	mm
Effective depth	d	450	mm
Concrete strength	f_{ck}	30	MPa
Steel modulus	E_s	200	GPa
Reinforcement ratio	ρ	0.30–2.00	%
Moment ratio	M_a/M_{cr}	1.00–4.00	—

3.2 Calculation procedure

For each reinforcement ratio, A_s, the modular ratio n, the neutral-axis depth x, I_g, and I_{cr} were computed. Each effective inertia was then obtained from Equations 5–7. Results were presented as normalized stiffness I_e/I_g and as the elastic deflection multiplier I_g/I_e. This multiplier corresponds to the ratio between the deflection computed with the selected effective inertia and the elastic deflection of the uncracked section, for any load case in which a single constant effective stiffness is used. Therefore, for a fixed λ, the relative comparison is independent of span and load magnitude.

Differences between models were assessed by the relative deflection index

$$D_{A/B} = 100\left[\left(\frac{\delta_A}{\delta_B}\right) - 1\right] = 100\left[\left(\frac{I_{e,B}}{I_{e,A}}\right) - 1\right] \tag{8}$$

where positive values indicate that ACI 318-19 predicts a larger immediate deflection than Branson. The same procedure was applied to the unreduced Bischoff formulation. The calculations were implemented in Python with double-precision arithmetic. The dataset in CSV format accompanies the analysis, and the preceding equations are sufficient for independent reproduction.

3.3 Limits of interpretation

The analysis is comparative, not a calibration. No experimental measurement was fitted, and no model is considered more accurate merely because it predicts a larger or smaller deflection.

Furthermore, the use of a single I_e in an elastic deflection equation is an equivalent-stiffness approximation; the actual curvature varies along the span as a function of moment and cracking. The results should therefore be interpreted as a sensitivity analysis of code-based calculations, not as a substitute

for nonlinear curvature integration or experimental validation. The 0.30% ratio was retained to examine the sensitivity of lightly reinforced sections and should not, by itself, be interpreted as demonstrating compliance with the minimum reinforcement requirements of any specific code.

4 RESULTS

4.1 Cracked-section stiffness

The ratio between the cracked and gross inertias increased monotonically with the reinforcement ratio (Table 2). The most lightly reinforced section therefore exhibited the greatest stiffness contrast and the greatest potential for divergence among the interpolation models. This result is important because the interpolation exponent does not govern divergence on its own: the ratio between section properties controls how much a difference in the retained tension-stiffening contribution affects total stiffness.

Table 2. Properties of the transformed cracked sections

ρ (%)	A_s (mm^2)	x (mm)	I_{cr}/I_g	I_g/I_{cr}
0.300	405.0	80.6	0.132	7.572
0.500	675.0	101.2	0.205	4.890
0.750	1012.5	120.4	0.285	3.504
1.000	1350.0	135.8	0.358	2.792
1.500	2025.0	159.8	0.486	2.056
2.000	2700.0	178.5	0.597	1.674

Figure 1 shows the common limiting behavior and the different transition paths. All models tend toward I_{cr} as λ increases. At low λ, Branson and the unreduced rational model start at I_g, whereas the ACI curve already lies below I_g at $M_a = M_{cr}$, since its transition is referenced to $(2/3)M_{cr}$. The separation is most visible for $\rho = 0.30\%$. For $\rho = 2.00\%$, the cracked inertia represents a much larger fraction of I_g, reducing the range over which the interpolations can diverge.

4.2 Deflection divergence

The contour map confirms that the largest effect occurs at the onset of the post-cracking regime and at low reinforcement ratios, with a maximum of 365% for $\rho = 0.30\%$ at $M_a = M_{cr}$. The ACI formulation yields a larger predicted deflection over almost the entire cracked domain investigated. The only exception occurs for $\rho = 2.00\%$ at $\lambda \geq 3.75$, where the Branson equation becomes marginally more flexible; the reversal is negligible in practice (at most 0.08%, at $\lambda = 4.00$).

The difference decreases in two directions: with increasing reinforcement, because I_{cr} approaches I_g, and with increasing load ratio, because all formulations approach I_{cr}. Model choice is thus most relevant precisely when the service load lies only moderately above the nominal cracking load.

Figure 3 isolates the effect of reinforcement for selected load levels. At $\lambda = 1.1$, the reduced cracking transition in ACI 318-19 produces a sharp increase in the computed deflection. At $\lambda = 3.0$ and 4.0, the curves flatten because the member response approaches the fully cracked limit. The monotonic trend is consistent with the interpretation of Bischoff and Scanlon (2007): the traditional Branson equation is less transferable outside the reinforcement range that dominated its original calibration.

4.3 Representative numerical comparisons

The representative values in Table 3 show that ACI 318-19 yields the lowest stiffness over almost the entire domain, and always lower stiffness than the unreduced Bischoff expression. The relative position

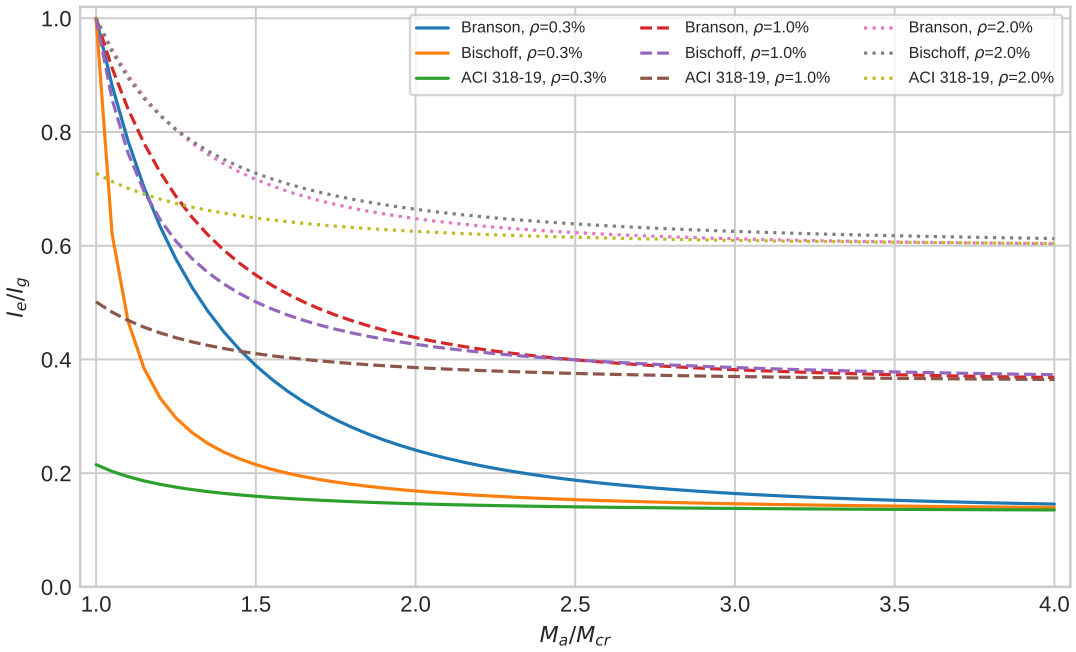


Figure 1. Normalized effective inertia as a function of the ratio between applied moment and cracking moment

of Branson and the unreduced Bischoff expression depends on the reinforcement ratio and load level.

For $\rho \leq 0.50\%$, Branson retains the highest stiffness at every load ratio investigated. For $\rho \geq 0.75\%$, the unreduced Bischoff expression becomes slightly stiffer than Branson beyond a load ratio that decreases with reinforcement (from $\lambda = 3.30$ for $\rho = 0.75\%$ to $\lambda = 1.25$ for $\rho = 2.00\%$), although the difference between the two remains below 2.6% in deflection terms. The exact percentage difference should not be generalized beyond the adopted geometry and material assumptions, but the trends are governed mainly by the dimensionless pairs M_a/M_{cr} and I_{cr}/I_g and can therefore be transferred to similar rectangular sections.

Table 3. Representative values of normalized stiffness and deflection differences

ρ (%)	M_a/M_{cr}	Branson I_e/I_g	Bischoff I_e/I_g	ACI I_e/I_g	ACI deflection above Branson (%)
0.30	1.10	0.784	0.467	0.194	304.46
0.30	1.50	0.389	0.215	0.159	144.19
0.30	2.00	0.241	0.169	0.146	64.58
1.00	1.10	0.840	0.763	0.469	79.30
1.00	1.50	0.548	0.501	0.410	33.68
1.00	2.00	0.438	0.427	0.386	13.67
2.00	1.10	0.900	0.895	0.701	28.37
2.00	1.50	0.717	0.727	0.649	10.43
2.00	2.00	0.648	0.664	0.625	3.58

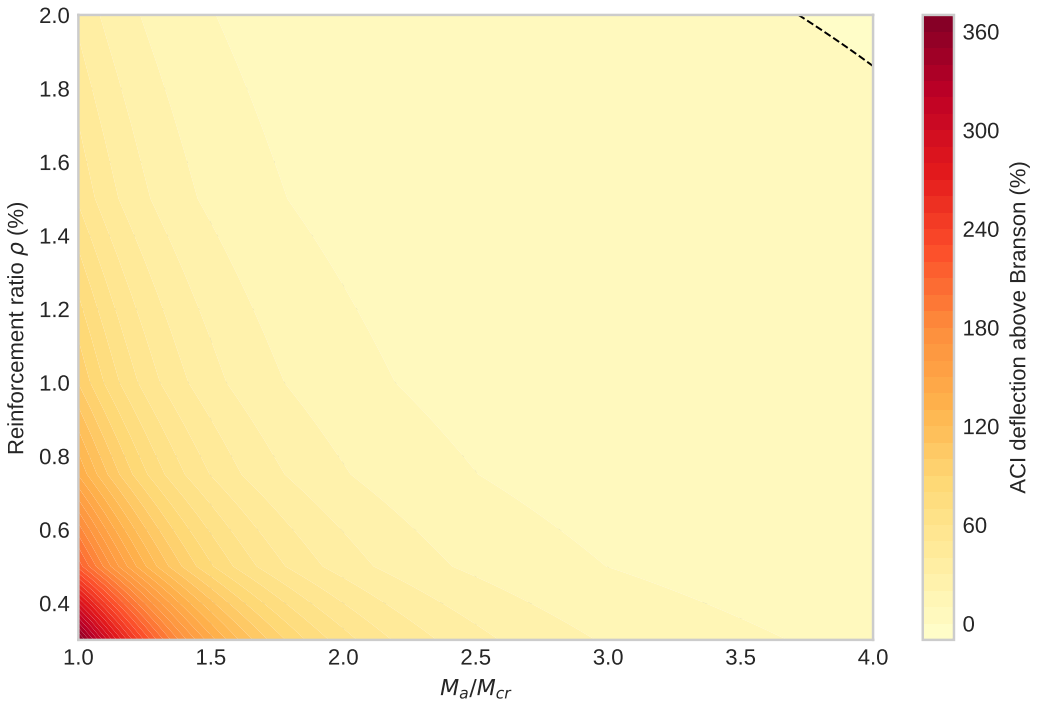


Figure 2. Increase in deflection predicted by ACI 318-19 relative to Branson. The dashed line marks the zero contour

5 DISCUSSION

5.1 Mechanical meaning of the differences

The three equations share the same physical limits but embody different assumptions about the contribution of concrete in tension. Branson interpolates the inertia directly through a cubic moment ratio. The rational formulation performs an interpolation more closely related to curvature and flexibility, making the stiffness contrast explicit. ACI 318-19 adds a separate practical adjustment by reducing the nominal cracking threshold.

This distinction matters: the difference between Branson and Bischoff concerns the mathematical representation of post-cracking stiffness, whereas the additional difference introduced by ACI concerns the point at which the transition is assumed to begin.

The pronounced response at low reinforcement can be explained without favoring any code. When A_s is small, the neutral axis of the transformed cracked section is shallow and I_{cr} is much smaller than I_g. A modest change in the participation of the gross section then produces a large proportional change in I_e. Conversely, as the reinforcement ratio increases, I_{cr} itself sets a higher lower bound on stiffness, reducing the influence of the interpolation.

5.2 Implications for design comparisons

Practitioners comparing calculations from different codes or software should not attribute all deflection discrepancies to numerical implementation. If one program applies a cubic Branson/NBR-type expression and another applies ACI 318-19, divergent results are expected even with identical geometry, reinforcement, modulus of elasticity, and loading. The discrepancy will be amplified in lightly reinforced beams and at loads close to cracking. A transparent report should therefore present at least M_{cr}, I_g, I_{cr}, and the adopted I_e equation, rather than only the final displacement.

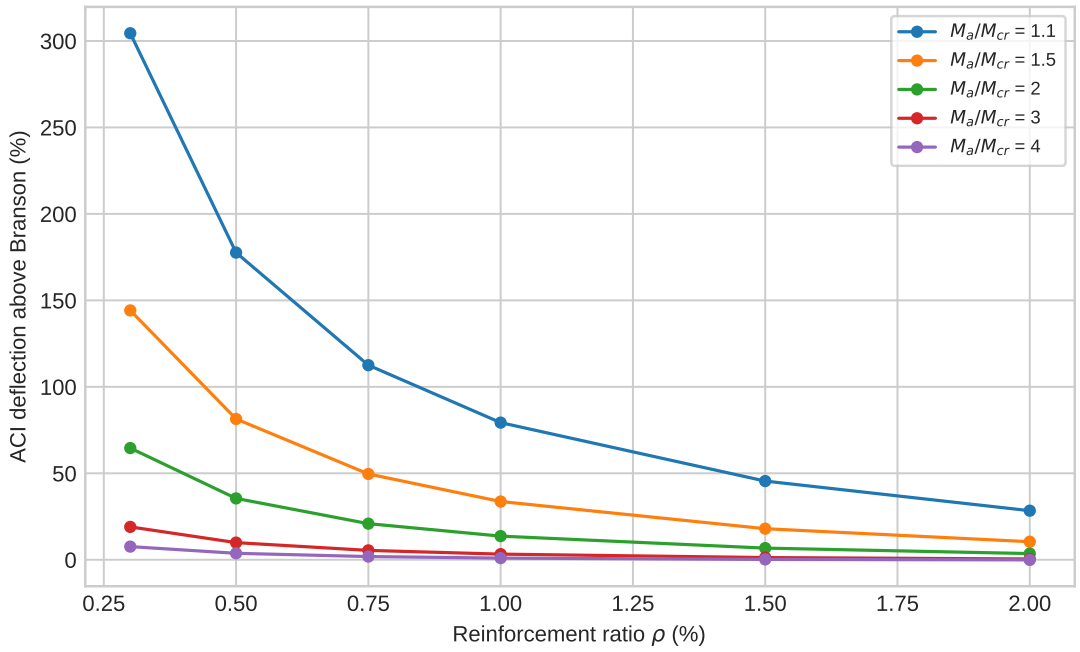


Figure 3. Sensitivity of the ACI–Branson deflection difference to the reinforcement ratio

The results also caution against automatically interpreting the more conservative prediction as the more accurate one. Reduced stiffness may, in some cases, compensate for unmodeled shrinkage restraint or tensile-strength variability, but accuracy depends on member type, reinforcement, load distribution, construction history, and the definition of the measurement. A defensible validation study should compare predicted load–deflection curves with individual experimental specimens and quantify bias and scatter, rather than ranking equations solely on theoretical results.

5.3 Relation to previous research

The parametric trends agree with the conclusions of Bischoff and Scanlon (2007), who found the Branson expression valid for steel reinforcement ratios greater than about 1% but prone to overestimating stiffness at lower ratios. Scanlon and Bischoff (2008) showed that deflections of lightly reinforced members (reinforcement ratio below 0.8%) are highly sensitive to shrinkage restraint cracking and loading history, whereas more heavily reinforced members are insensitive to these effects at full service load; this is consistent with the concentration of the ACI–Branson divergence at low reinforcement ratios found here.

Kalkan (2013) compared the Branson and Bischoff expressions with measured deflections of beams with reinforcement ratios between 2.4% and 3.4%, above the range studied here, and found close agreement with the measured values for most specimens, with the Bischoff expression performing slightly better. Although that range lies outside the present domain, the result is compatible with the trend of decreasing divergence with increasing reinforcement observed here. The same study reported that restrained shrinkage cracking made the measured response more flexible than either expression predicted.

Patel et al. (2015) derived an explicit expression for the effective inertia of uniformly loaded reinforced concrete beams from a neural network trained on finite-element results, accounting for cracking, tension stiffening, and the practical range of reinforcement. Other deflection prediction methods continue to be proposed, and effective-stiffness modeling remains an active serviceability problem.

Kim and Kim (2021), for example, incorporated the contribution of shear to the deflection of flexure-critical beams and reported that, for 60 beams compiled from the literature, ACI 318-19 underestimated

the measured deflections at first yielding of the tension reinforcement by approximately 33% (mean test-to-predicted ratio of 1.33). Because that comparison refers to flexural yield rather than service load, it is not directly comparable with the immediate service deflections examined here.

5.4 Limitations and next research step

Four limitations define the scope of this work. First, the analysis considers only immediate deflection; long-term deformations may dominate the total service displacement. Second, singly reinforced rectangular sections are used, without representing slabs, T-beams, compression reinforcement, or prestressing. Third, shear deformations and bond slip are omitted. Fourth, no experimental observations are used. The results therefore establish sensitivity and expected relative conservatism, but not statistical accuracy.

The logical next step is a pre-registered validation using an open database of tests on steel-reinforced concrete beams. Geometry, material properties, loading configuration, measured cracking load, and displacement should be preserved at the level of each specimen. Performance could then be assessed through the mean predicted-to-test ratio, coefficient of variation, mean absolute percentage error, and coverage of serviceability limits. Separating measured from computed M_{cr} would further make it possible to identify whether the error stems mainly from the cracking-load estimate or from the post-cracking stiffness interpolation.

6 CONCLUSIONS

A normalized parametric study was carried out to compare the Branson, rational Bischoff, and ACI 318-19 effective inertia models in the computation of the immediate deflection of reinforced concrete beams. Within the domain investigated, model choice had the greatest effect immediately after cracking and in lightly reinforced sections, where the I_g/I_{cr} ratio is largest. Because it combines rational interpolation with a reduced cracking moment, the ACI 318-19 formulation predicted lower effective stiffness and larger immediate deflection than Branson's cubic formulation over almost the entire cracked range; the only exception, for $\rho = 2.00\%$ at $M_a/M_{cr} \geq 3.75$, is a reversal below 0.1% with no practical significance.

The differences decreased with increasing M_a/M_{cr}, because all models approach the fully cracked inertia, and with increasing reinforcement ratio, as I_{cr} comes to represent a larger share of I_g. For reinforcement ratios near or above 1%, the divergence was smaller, consistent with the range in which previous experimental studies found the Branson equation reasonably applicable (Bischoff and Scanlon, 2007).

Deflection comparisons between codes or software should therefore report M_{cr}, I_g, I_{cr}, and the effective inertia equation, since the final displacement alone is insufficient to diagnose the divergence. Finally, the study does not identify the most accurate model; such a claim would require specimen-level experimental validation and uncertainty analysis.

REFERENCES

ABNT. (2023), *NBR 6118:2023: Projeto de estruturas de concreto* [Design of concrete structures]. Associação Brasileira de Normas Técnicas, Rio de Janeiro.

ACI Committee 318. (2019), *Building code requirements for structural concrete and commentary (ACI 318-19)*. American Concrete Institute, Farmington Hills, MI.

Al-Shaikh, A. H., Al-Zaid, R. Z. (1993), Effect of reinforcement ratio on the effective moment of inertia of reinforced concrete beams. *ACI Structural Journal*, 90(2):144–149. https://doi.org/10.14359/4119

Al-Zaid, R. Z., Al-Shaikh, A. H., Abu-Hussein, M. M. (1991), Effect of loading type on the effective moment of inertia of reinforced concrete beams. *ACI Structural Journal*, 88(2):184–190. https://doi.org/10.14359/2690

Bischoff, P. H. (2005), Reevaluation of deflection prediction for concrete beams reinforced with steel and fiber reinforced polymer bars. *Journal of Structural Engineering*, 131(5):752–767. https://doi.org/10.1061/(ASCE)0733-9445(2005)131:5(752)

Bischoff, P. H. (2007), Rational model for calculating deflection of reinforced concrete beams and slabs. *Canadian Journal of Civil Engineering*, 34(8):992–1002. https://doi.org/10.1139/L07-020

Bischoff, P. H., Scanlon, A. (2007), Effective moment of inertia for calculating deflections of concrete members containing steel reinforcement and fiber-reinforced polymer reinforcement. *ACI Structural Journal*, 104(1):68–75. https://doi.org/10.14359/18434

Branson, D. E. (1963), *Instantaneous and time-dependent deflections of simple and continuous reinforced concrete beams*. HPR Report No. 7, Part 1, Alabama Highway Department and Bureau of Public Roads, Auburn University, Auburn, AL. https://rosap.ntl.bts.gov/view/dot/42307

European Committee for Standardization. (2004), *EN 1992-1-1: Eurocode 2 — Design of concrete structures — Part 1-1: General rules and rules for buildings*. CEN, Brussels.

Gilbert, R. I. (1999), Deflection calculation for reinforced concrete structures — Why we sometimes get it wrong. *ACI Structural Journal*, 96(6):1027–1032. https://doi.org/10.14359/779

Kalkan, İ. (2013), Deflection prediction for reinforced concrete beams through different effective moment of inertia expressions. *International Journal of Engineering Research and Development*, 5(1). https://dergipark.org.tr/en/pub/umagd/article/346049

Kim, S.-W., Kim, K.-H. (2021), Prediction of deflection of reinforced concrete beams considering shear effect. *Materials*, 14(21):6684. https://doi.org/10.3390/ma14216684

Patel, K. A., Bhardwaj, A., Chaudhary, S., Nagpal, A. K. (2015), Explicit expression for effective moment of inertia of RC beams. *Latin American Journal of Solids and Structures*, 12(3):542–560. https://doi.org/10.1590/1679-78251272

Scanlon, A., Bischoff, P. H. (2008), Shrinkage restraint and loading history effects on deflections of flexural members. *ACI Structural Journal*, 105(4):498–506. https://doi.org/10.14359/19864

Scanlon, A., Murray, D. W. (1982), Practical calculation of two-way slab deflections. *Concrete International*, 4(11):43–50.